conf-780488--3

LA-UR -78-1624

TITLE:

FLOW-SYSTEM MEASUREMENT OF CELL IMPEDANCE PROPERTIES

AUTHOR(S):

MASTER

R. A. Hoffman and W. B. Britt

SUBMITTED TO:

In: Proceedings of the Sixth Engineering Foundation Conference on Automated Cytology, Elmau, West Germany (April 23-29, 1978), Brian H. Mayall, Ed. (Journal of Histochemistry and Cytochemistry)

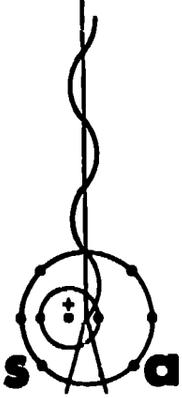

los alamos
scientific laboratory
of the University of California
LOS ALAMOS, NEW MEXICO 87545

Form No. 836
St. No. 2629
1/78

UNITED STATES
ENERGY RESEARCH AND
DEVELOPMENT ADMINISTRATION
CONTRACT W-7405-ENG. 36

Running title: Cell Impedance Properties

FLOW-SYSTEM MEASUREMENT OF CELL IMPEDANCE PROPERTIES

R. A. Hoffman and W. B. Britt

Biophysics and Instrumentation Group, Los Alamos Scientific Laboratory, University of California Los Alamos, New Mexico 87545

Received for publication _____, 1978

Send proofs to: Dr. R. A. Hoffman
Biophysics and Instrumentation Group (MS888)
Los Alamos Scientific Laboratory
University of California
Los Alamos, New Mexico 87545

SUMMARY

A flow-system technique has been developed that detects the high-frequency resistance and capacitance changes in a sensing orifice due to the passage of cells through the orifice. The resistance and capacitance changes are related to cell properties such as size, plasma membrane capacitance, and electrical resistivity of the cell interior. The relationship between measured impedances and cellular properties is discussed, and the prototype instrument for making such measurements is described. The instrument can simultaneously detect the dc Coulter volume and two ac parameters related to the complex ac impedance change. Some initial tests of the instrument using plastic microspheres and Chinese hamster ovary cells are described.

For more than 50 years, measurements of the electrical impedance of cell suspensions have been used to probe the structure and composition of cells. The Coulter volume measurement, which was the first parameter to be used for the flow-system analysis of cells (6), is an impedance measurement at zero frequency (dc) or a measure of resistance. If the impedance measurement is made using an alternating electrical current of high frequency, it yields information that is much richer than the "volume" measured in the dc instance. We have developed a technique for making high-frequency impedance measurements on individual cells in a flow system. The purpose of this paper is to describe the technique and to give some insight into what information about cellular properties may be expected from the measurements. We will first discuss the basic impedance properties of cell suspensions and indicate the relationship between certain cellular properties and the impedance of the cell suspension. We will then describe the basic technique we use to make impedance measurements in a flow system and will discuss the electronics used in our detection scheme. Finally, we will discuss some preliminary results obtained with the present instrument.

IMPEDANCE PROPERTIES OF CELL SUSPENSIONS

We will consider the cell suspension impedance to be represented by a parallel combination of a resistance, R, and a capacitance, C. The impedance, Z, of the combination is $Z = \frac{R}{1 + j\omega RC}$, where $j = \sqrt{-1}$ and $\omega = 2\pi \times$ frequency. The admittance, A, is given by $A = 1/Z = 1/R + j\omega C$. It will usually be most convenient to consider the resistance and capacitance separately rather than the impedance. There are several good reviews of biological impedance properties (3,19-21), and we will present here only some basic ideas that will serve to introduce the subject. A suspension of cells can be represented electrically by an RC network with one or more time constants (19). This means that the resistance and capacitance of the suspension are functions of frequency.

The basis for this frequency dependence can be illustrated with a simple model. We will consider a cell to be composed of a uniform, homogeneous, spherical cytoplasm surrounded by a thin, nonconducting membrane. Although the cell membrane is considered to have no conductance (a situation very well approximated by normal cells), it has a rather large capacitance per unit area, C_M. Thus, at dc or low frequency, the cell appears electrically to be a perfect insulator, indistinguishable from a plastic sphere of the same size and shape, but at high frequencies, the membrane is shorted out and is electrically "invisible." The cell appears then as a sphere of cytoplasm. Figure 1a shows how the resistance and capacitance of a suspension of the model cells vary with frequency. The calculations are based on a theory by Pauly and Schwan (15,16), and the relevant equations are given in the appendix. To eliminate geometrical factors, the results are plotted as conductivity (proportional to $\frac{1}{\text{resistance}}$) and dielectric constant (proportional to capacitance). Both the conductivity and dielectric constant are essentially constant when the frequency is either very high or very

low, compared to a characteristic frequency, f_o. f_o is defined as the frequency where the sigmoid-shaped curve has its midpoint.

The low-frequency conductivity is the impedance parameter detected in the Coulter volume measurement. If the plasma membrane is nonconducting, the low-frequency conductivity, k_o, depends only on the relative volume of the cell. The low-frequency dielectric constant, ε_o, is primarily due to the plasma membrane capacitance, C_M. It is proportional to C_M and to the fourth power of the cell diameter, D. The high-frequency conductivity, k_∞, is determined by the resistivity, ρ_i, of the cell interior as well as the relative volume. The high-frequency dielectric constant, ε_∞, is determined by the dielectric constant of the cell interior, ε_i, and the relative volume. In a flow system, the relative volume is proportional to the volume of a single cell. For the spherical model cell, the Coulter volume measurement, or k_o, thus gives the volume and diameter of the cell. If ε_o is determined simultaneously with the Coulter volume, then C_M is determined. If k_∞ and k_o are determined simultaneously, then ρ_i is determined. If ε_∞ and k_o are determined simultaneously, then the internal dielectric constant of the cell is determined. It is important to note that the characteristic frequency, f_o, depends on several factors and is inversely proportional to both C_M and cell diameter, D. Figure 1b shows the change in a flow-system orifice impedance due to entry of the model cell. Note that the reactance change is a maximum at the characteristic frequency. In principle, it is possible to determine D, C_M, ρ_i, and ε_i by simultaneously measuring the cell impedance at extremes of low and high frequency. In practice, cell impedance measurements are complicated by internal cell structure and nonspherical shape, but the impedance at low- and high-frequency extremes will still depend on cellular properties such as C_M and ρ_i in much the same way as does the simple model discussed above.

Some idea of the range of cellular impedance properties may be obtained from Table I. In most cases shown, the cellular properties were determined from static impedance measurements on suspensions of cells. The membrane specific capacitance is often considered to have a constant nominal value of 1 $\mu F/cm^2$, but experimental values for various cell types range from 0.8 to 2.8 $\mu F/cm^2$. Cell membrane resistance is quite large for normal cells and generally may be considered infinite if the specific resistance is greater than 100 ohm-cm^2. The resistivity of the cell interior is always greater than that of normal saline (resistivity = 67 ohm-cm), but the experimental values lie in quite a large range of 77 to 556 ohm-cm. The internal resistivity is a function of macromolecule concentration and possibly internal structure and other factors. The dielectric constant of the cell interior is usually less than that of saline (dielectric constant = 78), although it may appear to be larger if internal structures such as the nucleus are sufficiently large and nonconducting. The wide variation in cellular parameters such as C_M and ρ_i suggest that cell impedance properties may be useful parameters for cell classification and analysis in flow systems.

MATERIALS AND METHODS

The basic method for measuring the ac impedance of cells is simply an extension of the Coulter volume technique. An ac current is made to flow through a small saline-filled orifice and, when a cell enters the orifice, the impedance across the orifice and the voltage across the orifice change. In general, both the amplitude and phase of the ac voltage across the orifice change and reflect the complex impedance change due to entry of the cell. Instruments have been built by Toa Electric Co., Ltd., and Coulter Electronics, Inc., which detect either the ac phase or the amplitude changes produced by cells in a sensing orifice. The Toa instrument is apparently designed to detect phase changes (11), while the prototype Coulter instrument detects amplitude changes (23). In the Coulter instrument, the ac amplitude change is divided by the dc amplitude change to yield a parameter called "opacity" (23). The "opacity" has been correlated with cell buoyant density (23) and with changes in cell populations after immunization to tumor cells (24).

Our approach differs from previous ones in that we use phase-sensitive detection to obtain the complete complex voltage change produced by a cell passing through the orifice. Since we want to detect both the resistance and capacitance changes in orifice impedance, our circuit has been arranged so that one detector will have an output proportional to the resistance change, while a second detector will have an output proportional to the capacitance change. A simplified schematic of the detector scheme is shown in Fig. 2. The sensing orifice is part of a bridge circuit. A steady ac signal is applied across nodes C and D. In our first experiments, node D has been grounded. A change in the sensing orifice impedance causes a change in the voltage at node A. When the bridge is balanced, the steady signals at nodes A and B

are equal, and the differential amplifier output is only the transient change at node A due to a transient change in the sensing orifice impedance. One can think of the voltage at node A as a carrier signal upon which a modulation is produced by changes in the sensing orifice impedance. When cells pass through the sensing orifice, they produce an asynchronous pulse modulation. The purpose of the remainder of the circuit is to demodulate the signal into two components that are 90° out of phase. In terms of ac circuit theory, the signal is demodulated into the two separate components of its complex amplitude. In our first experiments, we have used an inductor, L, to tune out the sensing orifice capacitance and a similar reactance network, X, is tuned for infinite reactance at bridge balance. Thus, at the frequency, f, of the ac voltage applied across nodes C and D, all the impedance elements in the bridge can be made nearly pure resistors. It can be shown that, under these conditions, the change in voltage at node A due to a small capacitance change, ΔC, and small resistance change, ΔR, in the sensing orifice has two components given by:

$$\Delta V\ (0°) = \frac{R'E}{(R_o + R')^2}\,\Delta R_o$$

$$\Delta V\ (90°) = \frac{-2\pi\, fR'R_o^{\,2}E}{(R_o + R')^2}\,\Delta C_o$$

where ΔV (0°) and ΔV (90°), respectively, are the changes in voltage that are in phase and 90° out of phase (quadrature) relative to the voltage across nodes C and D. E is the amplitude of the voltage applied across nodes C and D. Thus, separate signals can be obtained that are proportional to the resistance and capacitance changes in the orifice.

The bridge output usually has been detected with a differential amplifier. An NE592 integrated circuit with a FET buffered input has been used for this purpose. A reference signal is obtained through a similar amplifier which compensates for the phase shift in the differential amplifier. Thus, the phase is referenced to the bridge driving voltage between nodes C and D. A 90° phase shifted reference is obtained with a standard operational amplifier circuit (10). The product or synchronous detectors use an MC1596 balanced modulator integrated circuit. The detector sensitivity is approximately 2 μV, and the linear input range is 0 to 100 mV RMS. The detectors are phase-sensitive with the demodulated output proportional to $COS\phi$, where ϕ is the phase difference between the signal and reference input voltages. Rather, conventional ac coupled amplifiers with bandwidths of approximately 1 to 100 kHz amplify the demodulated signals to levels appropriate for pulse-height analysis.

The flow system is shown in Fig. 3. It uses a single sheath stream to constrain the sample stream to the center of the sensing orifice. The flow cell contains two pairs of electrodes. The large platinum electrodes shown in Fig. 2 are used to pass a dc current through the orifice. A separate pair of electrodes is located in the sensing orifice assembly. One configuration used for the orifice assembly is shown in Fig. 4. This type of sensing orifice is constructed using thick film hybrid circuit techniques. The sensing orifice electrodes are connected to nodes A and D of the bridge circuit, as shown in Fig. 2. They serve to pass the ac current into the sensing orifice and may be used also to detect the dc Coulter volume signal when a dc current is passed through the sensing orifice by the external electrodes. When dc Coulter volume is detected simultaneously with the ac parameters, a small

capacitor is placed in series with inductor, L, to prevent a dc short circuit. The dc Coulter volume signal is separated from the ac signals using simple low-pass and high-pass filters at the output of the differential amplifier. The filters are not shown in Fig. 2.

Our instrument is still in the developmental stage, and we do not intend to discuss construction details because they may change in the near future. Rather, we wish to point out certain problems associated with making ac measurements in a flow system. A major problem that affects the ac measurements is noise in the radio-frequency signal generator. An erythrocyte in an orifice 100 μm in diameter by 250 μm in length produces a modulation on the detector signal of the order of 0.001%. A good commercial signal generator may have a noise level of 0.01% in a band 100 kHz removed from the carrier frequency. Thus, some means of reducing this noise level is necessary if one is to obtain good resolution. The means we have chosen is the bridge circuit, which provides common-mode rejection. The bridge also reduces the steady voltage or "carrier" applied to the detector and thus reduces the dynamic range required of the detector. It is important to note that, if the bridge is to provide rejection of noise as well as the carrier, the bridge must be balanced not only at the carrier frequency but also in a band above the carrier which contains the modulation. In our case, we require that the bridge be balanced in a band 100 kHz above the carrier frequency. One way to obtain balance over a wide frequency range is to make the bridge as symmetrical as possible. In practice, it has been relatively easy to reduce the radio-frequency generator noise by a factor of 10 to 100, and the carrier can be made insignificant. It has not been possible, however, to null out the harmonics of the carrier frequency.

A second limitation is the voltage which may be applied to the differential amplifier. If the radio-frequency generator is transformer-coupled to nodes C and D, then any one of the nodes may be grounded. If nodes C and D are left floating and node A or B is grounded, then the differential amplifier can be replaced with a single-ended one whose input signal is the difference in voltage between nodes A and B.[1] This difference in voltage can be made quite small if the bridge is near balance. A transformer is also an inexpensive means to increase the voltage applied to the circuit.

A further problem is reduction of the modulation signal due to conductive paths shunting the sensing orifice at high frequencies. These shunting paths essentially add a resistance in parallel with the orifice resistance, R_o, and reduce the actual impedance change between nodes A and D of the bridge, compared to the impedance change in the sensing orifice. The reasons for this additional conductive path in our present flow cell are not known. Both capacitively coupled conductive paths and dielectric losses in the flow cell probably contribute. Placing the sensing electrodes within or very near the sensing orifice minimizes this problem, but at present this is the major limitation that has prevented our using frequencies higher than a few MHz.

RESULTS AND DISCUSSION

The present instrument can detect both resistive (0° detector) and capacitive (90° detector) impedance changes due to typical mammalian cells. The signals from the 90° detector, however, generally have been too near the noise level to permit useful pulse-height analysis with this parameter. It has been possible to perform pulse-height analyses on the dc Coulter volume signal and the 0° ac parameter, which are detected simultaneously. Polystyrene microspheres and Chinese hamster ovary (CHO) cells have been used in initial tests of instrument capabilities. Figure 5 shows pulse-height spectra of the dc Coulter volume and the 0° ac parameter for 15.7-μm diameter polystyrene microspheres and CHO cells. For this experiment, the circuit configuration shown in Fig. 2 was used with node D of the bridge grounded. The frequency of the radio-frequency generator was 1.00 MHz, and the voltage applied across nodes C and D was 3 V RMS. The sensing orifice shown in Fig. 3 was used. All measurement conditions were identical for the experiments with the polystyrene spheres and CHO cells. The dc and ac parameters for each event were obtained simultaneously and stored in a computer using the data acquisition system for the LASL Sorter II multiparameter cell sorter (18). Standard LASL software (18) was used for subsequent data analysis. The signal-to-noise ratio was generally 10:1 or better for the dc parameter, and no noise peak appeared in the distributions of the dc parameter. Noise is a greater problem for ac measurements and is substantial in channels 9 and below.

The resolution of the instrument was just sufficient to allow a reasonable pulse-height spectrum to be obtained for CHO cells, whose mean diameter is approximately 12.5 μm. Figure 6 shows the data from Fig. 4a and 4b presented in a two-parameter contour plot. Most events are from CHO cells, but a

subpopulation shown in the crosshatched region is due to a small (0.3%) contamination of 15.7-μm polystyrene spheres that were not completely flushed out after a previous experiment.

There is a high correlation between the 0° ac and dc parameters for CHO cells. This is not unexpected at the relatively low frequency used. There were several poorly resolved minor peaks in the two-parameter contour plot, but they have not been interpreted. Additional experiments with CHO cells have shown that the peak of the 0° ac distribution shifts to higher channels as the ac frequency is decreased from 1.0 to 0.7 MHz. This is expected, since the resistance change produced by the cell is expected to increase as the frequency is decreased (see Fig. 1b).

Some recent experiments with different circuit configurations have enabled us to increase instrument resolution. A broadband transformer was used to couple a radio-frequency generator to the bridge, and nodes C and D shown in Fig. 2 were floated above ground. The transformer also stepped up the voltage applied to the bridge from 3 to 9 V RMS. Node B was grounded and a single-ended amplifier connected between node A and the product detectors. The reference voltage was taken from the primary of the transformer. Pulse-height spectra of the 0° ac parameter for 7.8-μm diameter polystyrene microspheres were obtained using a sapphire sensing orifice 91 μm in diameter and 250 μm in length. The signal-to-noise ratio was 3:1, and the coefficient of variation was 12% at a frequency of 1.2 MHz. This resolution would be sufficient to detect 7-μm spheres in a 91-μm diameter by 250-μm long orifice.

The high-frequency resistance and capacitance measurements of cells have the potential to be unique, new parameters for flow-system analysis of single cells. A method has been described which, with technical improvements, can

make such measurements on a wide range of cell types. It will be possible in the near future to begin exploring possible applications in biology and clinical cytology.

ACKNOWLEDGMENT

This work was performed under interagency agreement YO1-CM-40102 between the United States Department of Energy and the National Cancer Institute of the National Institutes of Health.

FOOTNOTE

[1]We thank W. H. Coulter and W. R. Hogg for this suggestion.

APPENDIX

Impedance of a Suspension of Spherical Cells

The simplest, realistic model for a cell is a uniform homogeneous cytoplasm surrounded by a thin membrane. Pauly and Schwan (16) have determined the electrical impedance of a suspension of spherical cells with these properties. If the membrane of the cell is essentially nonconducting, then the following equations result (15).

$$\varepsilon_o = \frac{1 - p/2}{1 + p} \varepsilon_s + \left(\frac{9}{8 \varepsilon_r}\right) \left(\frac{p}{p + 1}\right) DC_M \tag{A1}$$

$(\varepsilon_r = 8.85 \times 10^{-14}$ Farad/cm)

$$\varepsilon_\infty = \varepsilon_s \frac{(1 + 2p)\, \varepsilon_i + 2(1 - p)\, \varepsilon_s}{(1 - p)\, \varepsilon_i + (2 + p)\, \varepsilon_s} \tag{A2}$$

$$k_o = k_s \left[(1 - p)/(1 + p/2)\right] \tag{A3}$$

$$k_\infty = k_s \frac{1 + 2p\, (k_i - k_s)/(k_i + 2k_s)}{1 - p\, (k_i - k_s)/(k_i + 2k_s)} \tag{A4}$$

$$f_o = \left[\pi\, DC_M \frac{k_i + 2k_s}{2k_i\, k_s}\right]^{-1} \tag{A5}$$

where ε_o and k_o are the values of dielectric constant and conductivity in the low-frequency limit, ε_∞ and k_∞ are the values in the high-frequency limit, p is the volume fraction of the cells, C_M is the membrane specific capacitance, ε_i and ε_s are the dielectric constants of the cytoplasm and external medium, respectively, and k_i and k_s are the conductivities of the cytoplasm and external medium, respectively. D is the cell diameter. The membrane resistance is

assumed to be infinitely large. The dielectric constant and conductivity of the cell suspension at an arbitrary frequency, f, are given by:

$$\varepsilon = \varepsilon_\infty + [\varepsilon_o - \varepsilon_\infty]/[1 + (f/f_o)^2]$$

$$k = k_\infty + [k_o - k_\infty]/[1 + (f/f_o)^2]$$

f_o is called the characteristic frequency. The equations apply equally well to a suspension of a single cell or a suspension of many identical cells.

LITERATURE CITED

1. Asami K, Hanai T, Koizumi N: Dielectric properties of yeast cells. J Membr Biol 28:169, 1976
2. Carstensen EL: Passive electrical properties of microorganisms. II. Resistance of the bacterial membrane. Biophys J 7:493, 1967
3. Cole KS: Membranes, Ions, and Impulses. University of California Press, Berkeley, 1968, p 6-59
4. Cole KS, Curtis HJ: Electric impedance of single marine eggs. J Gen Physiol 21:591, 1938
5. Cole KS, Guttman RM: Electric impedance of the frog egg. J Gen Physiol 25:765, 1942
6. Coulter WH: High speed automatic blood cell counter and cell size analyzer. Proc Natl Electron Conf 12:1034, 1956
7. Fricke H: The electric capacity of suspensions with special reference to blood. J Gen Physiol 9:137, 1925
8. Fricke H: The electric conductivity and capacity of disperse systems. Physics 1:106, 1931
9. Fricke H, Curtis HJ: Electric impedance of suspensions of leukocytes. Nature 135:436, 1935
10. Graeme JG: Applications of Operational Amplifiers, Third-Generation Techniques. McGraw-Hill Book Co., New York, 1973, p 102-103
11. Helleman PW, Benjamin CJ: The Toa microcell counter. I. A study of the correlation between the volume of erythrocytes and their frequency distribution curve. Scand J Haematol 6:69, 1969
12. Irimajiri A, Doida Y, Hanai T, Inouye A: Passive electrical properties of cultured murine lymphoblast (L5178Y) with reference to its cytoplasmic

membrane, nuclear envelope, and intracellular phases. J Membr Biol 38:209, 1978

13. Kanno Y, Ashmen RF, Loewenstein WR: Nucleus and cell membrane conductance in marine oocytes. Exp Cell Res 39:184, 1965

14. Malenkov AC, Bogatyreva SA, Boshkova VP, Modjanova EA, Vasiliev JuM: Reversible alterations of the surface of ascites tumor cells induced by a surface-active substance Tween 60. Exp Cell Res 48:307, 1967.

15. Pauly H: Uber die elektrische Kapazitat der Zellmembran und die Leitfahigkeit des Zytoplasmas von Ehrlich-Aszitestumorzellen. Biophysik 1:143, 1963

16. Pauly H, Schwan HP: Uber die Impedanz einer Suspension von kugelformigen Teilchen mit einer Schale. Z Naturforsch 14B:125, 1959

17. Pauly H, Schwan HP: Dielectric properties and ion mobility in erythrocytes. Biophys J 6:621, 1966

18. Salzman GC, Hiebert RD, Crowell JM: Data acquisition and display for a high-speed cell sorter. Comput Biomed Res 11:77, 1978

19. Schwan HP: Electric properties of tissues and cell suspensions. Adv Biol Med Phys 5:147, 1957

20. Schwan HP: Alternating current spectroscopy of biological substances. Proc IRE 47:1841, 1959

21. Schwan HP: Determination of biological impedances, in Physical Techniques in Biological Research. Edited by W. L. Nastuk. Academic Press, Inc., New York, 1963, Vol. 6, p 323

22. Schwan HP, Morowitz HJ: Electrical properties of the membranes of the pleuropneumonia-like organism A5969. Biophys J 2:395, 1962

23. Thomas RA, Yopp TA, Watson BD, Hindman DHK, Cameron BF, Leif SB, Leif RC, Roque L, Britt W: Combined optical and electrical analysis of cells with the AMAC transducers. J Histochem Cytochem 25:827, 1977

24. Thornthwaite JT, Sugarbaker EV, Britt WB, Leif RC, Hudson JL: Cytophysical, biochemical and immunological analysis of the immune response against allogenic tumor cells. Edited by E. M. Sullivan. Poster Presentations at the Fifth Engineering Foundation Conference on Automated Cytology, Los Alamos Scientific Laboratory report LA-6719-C, 1977, p 4

TABLE I

Electrical Properties of Cells Assuming Homogeneous Cell Interior

	Cell type	Plasma Membrane Specific Capacitance, C_M ($\mu F/cm^2$)	Plasma Membrane Specific Resistance, R_M ($ohm\text{-}cm^2$)	Cell Interior Resistivity, ρ_i (ohm-cm)	Cell Interior Dielectric Constant ε_i	Reference
1.	Pleuropneumonia-like organism	1.30		100		(22)
2.	*Escherichia coli*	1.00		333		(2)
3.	Beef erythrocyte			230	51.3	(17)
4.	Dog erythrocyte	0.81				(7)
5.	Human erythrocyte	0.80				(8)
6.	Human erythrocyte			193	50.1	(17)
7.	Yeast	1.10		330	50.0	(1)
8.	Frog egg	2.00	170	570		(5)
9.	Asterias egg		860			(13)
10.	Arbacia egg (unfertilized)	1.10		180		(4)
11.	Arbacia egg (fertilized)	2.80		210		(4)
12.	Rabbit leukocyte	1.00		140		(9)
13.	Ehrlich-ascites tumor	2.00		77	> 70.0[a]	(15)
14.	Ehrlich-ascites tumor		1			(14)
15.	Mouse lymphoblast	0.98	~ 1000	155	139.0	(12)
16.	Chinese hamster ovary	1.55		117		(b)

[a] Based on datum $\varepsilon_o = 70$ and estimate $\varepsilon_a > 70$.

[b] Hoffman RA: unpublished data. The data are averaged for cells examined in various parts of the cell cycle.

FIG. 1. Impedance properties of a model spherical cell according to the Pauly-Schwan theory (15). The cell properties are diameter = 20 μm, C_M = 1 μF/cm^2, ε_i = 100, ρ_i = 100 ohm-cm. The saline electrical properties are ε_{saline} = 80 and ρ_{saline} = 67 ohm-cm. (a) Dielectric constant and conductivity of normal saline and a 1% (by volume) suspension of the model cells in normal saline; and (b) percentage change in an orifice resistance and reactance due to entry of the model cell. The model cell occupies 1% of the orifice volume.

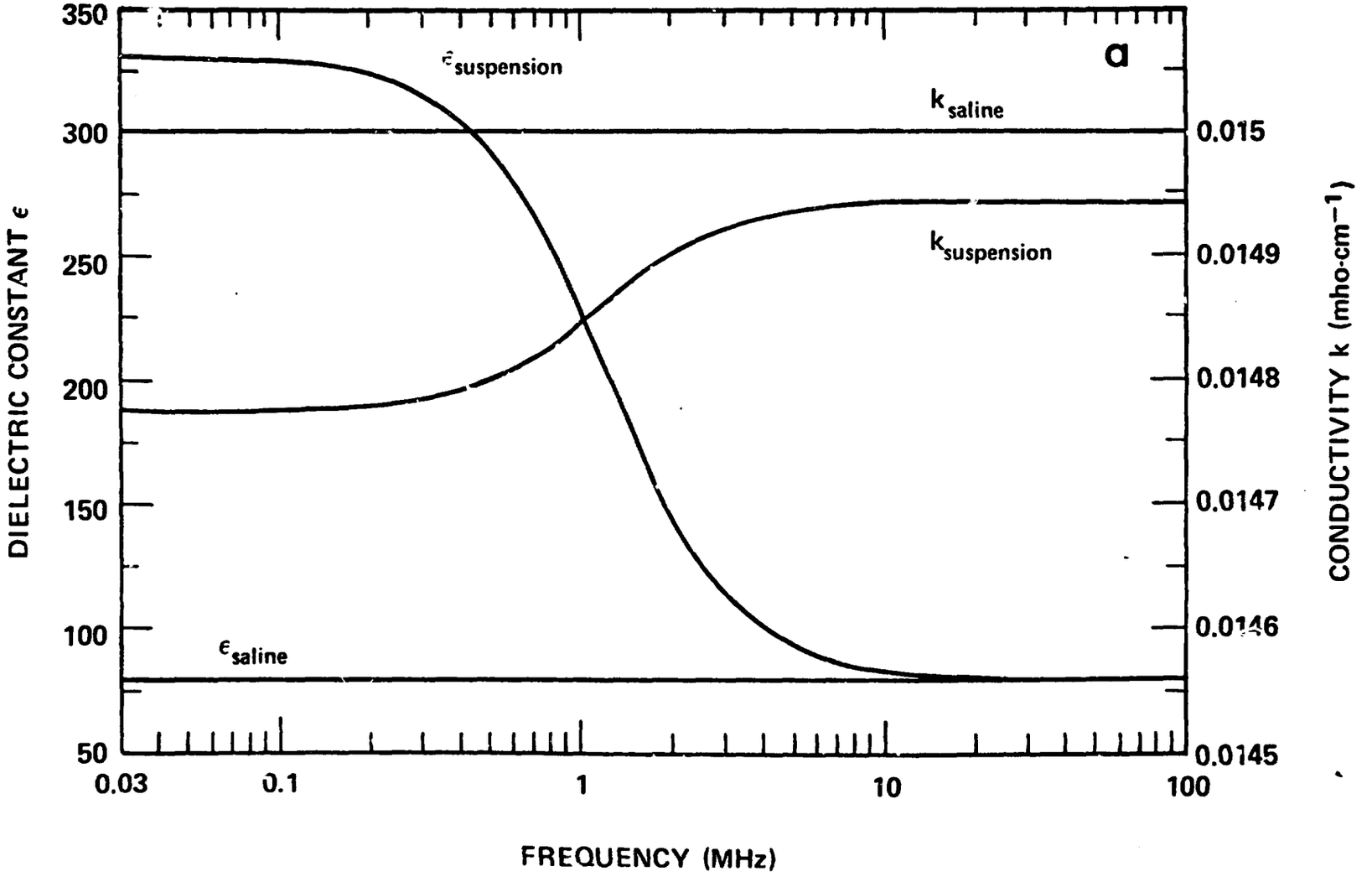
a
$\epsilon_{suspension}$
k_{saline}
$k_{suspension}$
ϵ_{saline}
350
300
250
200
150
100
50
0.03
0.1
1
10
100
0.015
0.0149
0.0148
0.0147
0.0146
0.0145
DIELECTRIC CONSTANT ϵ
CONDUCTIVITY k (mho-cm^{-1})
FREQUENCY (MHz)

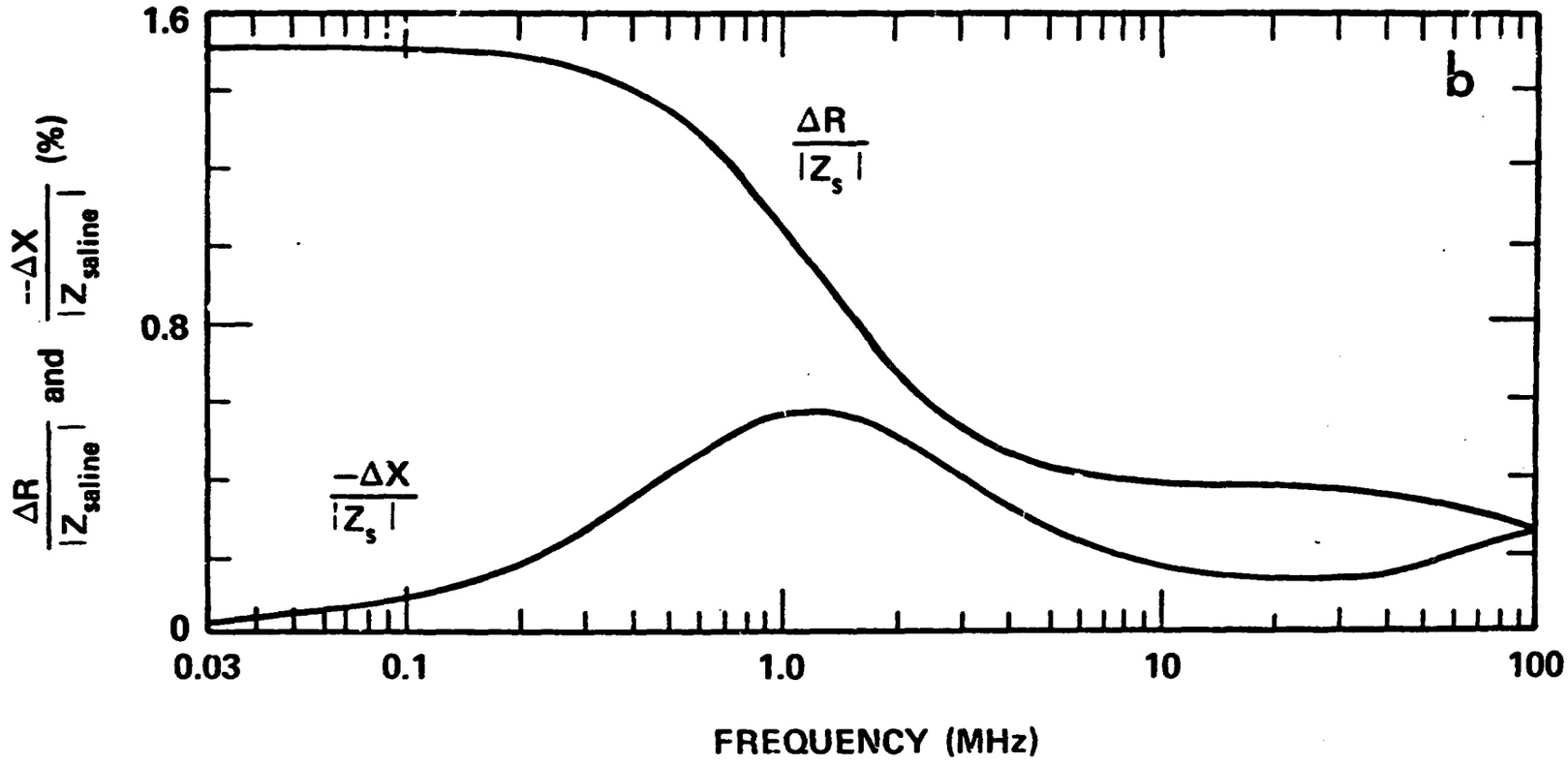
1.6
0.8
0
0.03
0.1
1.0
10
100
b
$\frac{\Delta R}{|Z_s|}$
$\frac{-\Delta X}{|Z_s|}$
$\frac{\Delta R}{|Z_{saline}|}$ and $\frac{-\Delta X}{|Z_{saline}|}$ (%)
FREQUENCY (MHz)

FIG. 2. Simplified schematic of phase-sensitive detector scheme.

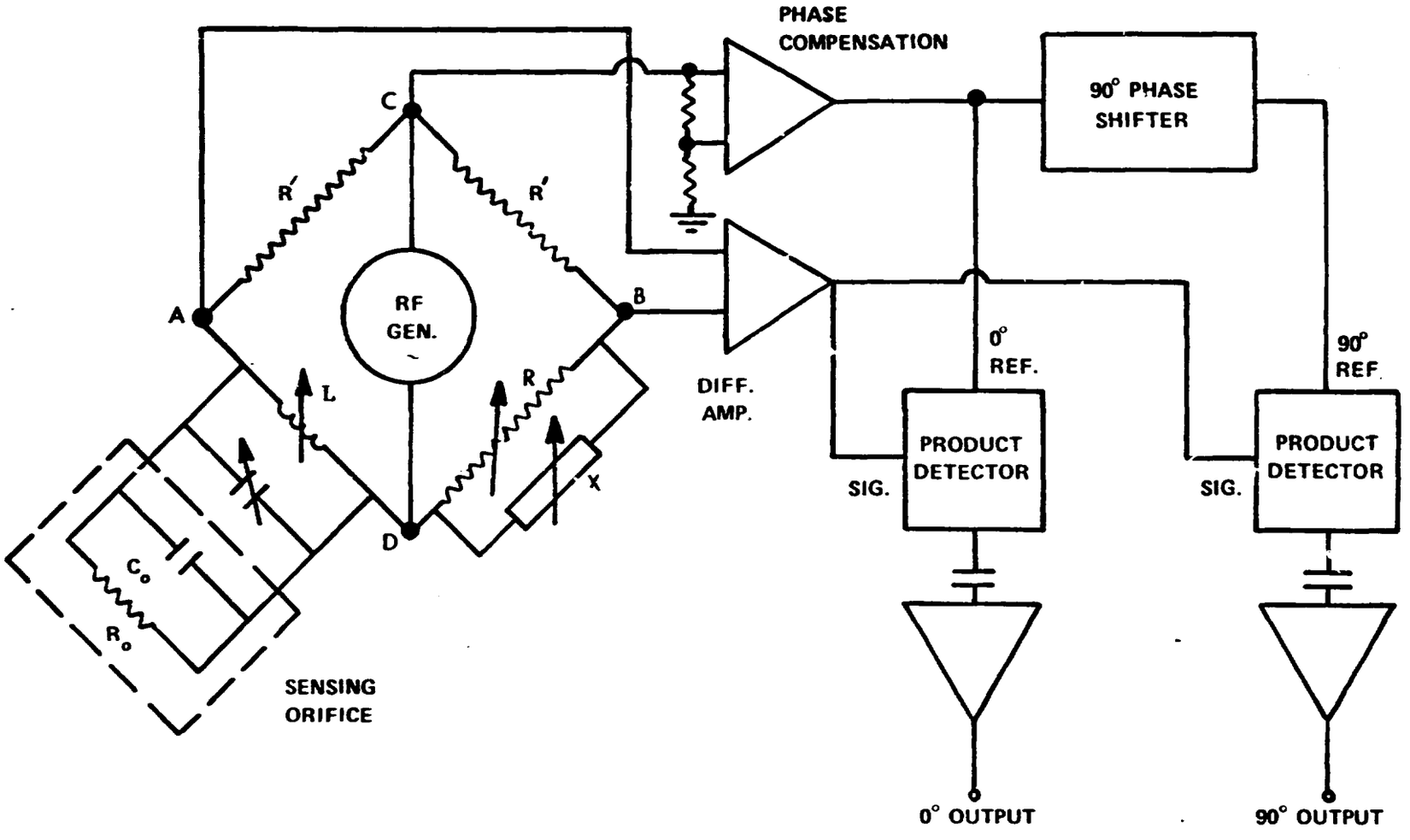
PHASE
COMPENSATION
90° PHASE
SHIFTER
C
R'
R'
A
RF
GEN.
B
L
R
X
D
DIFF.
AMP.
0°
REF.
90°
REF.
PRODUCT
DETECTOR
PRODUCT
DETECTOR
SIG.
SIG.
C_o
R_o
SENSING
ORIFICE
0° OUTPUT
90° OUTPUT

FIG. 3. Schematic of the flow system (flow chamber not to scale).

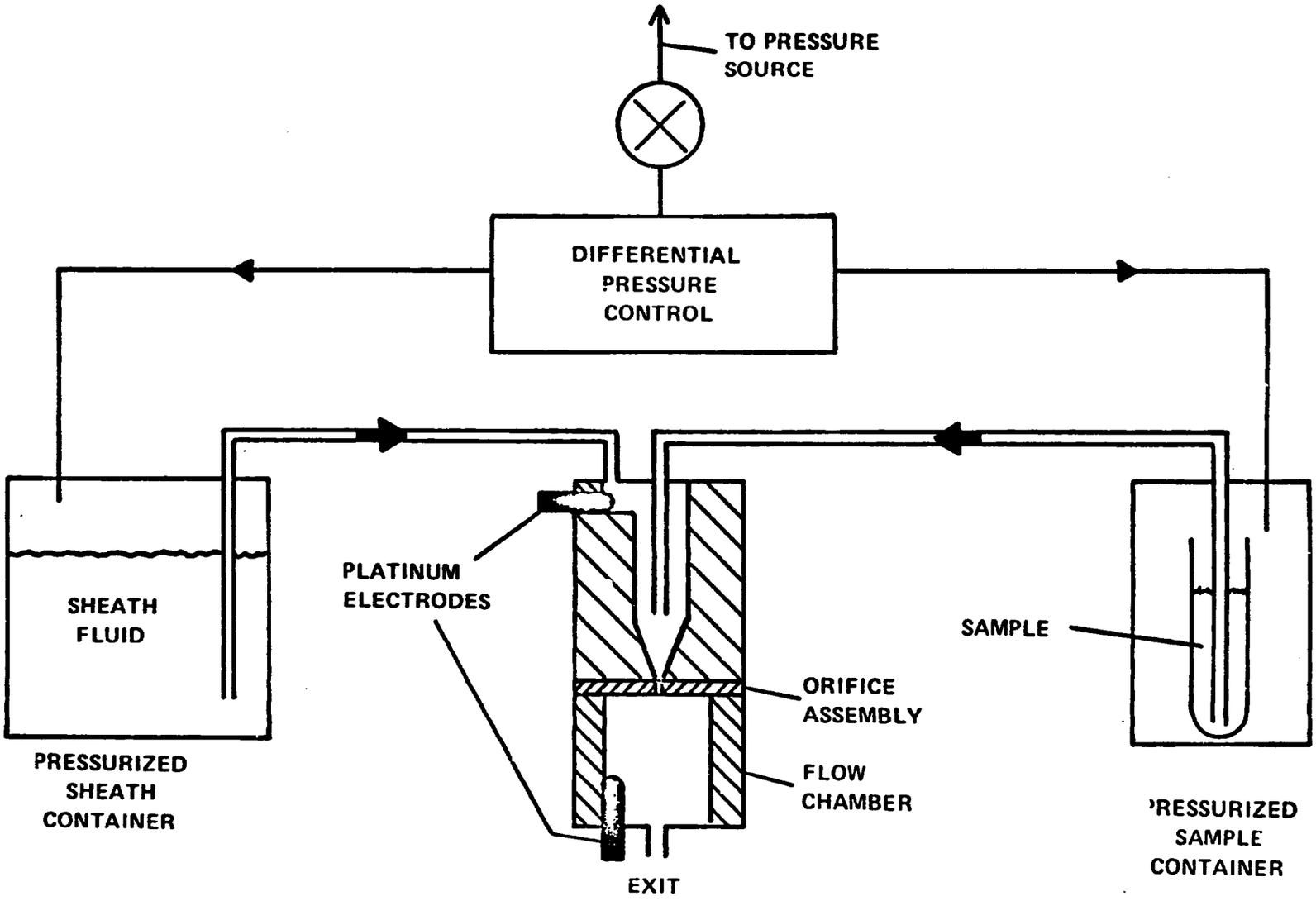
TO PRESSURE SOURCE
DIFFERENTIAL PRESSURE CONTROL
SHEATH FLUID
PRESSURIZED SHEATH CONTAINER
PLATINUM ELECTRODES
ORIFICE ASSEMBLY
FLOW CHAMBER
EXIT
SAMPLE
PRESSURIZED SAMPLE CONTAINER

FIG. 4. Sensing orifice: (a) electrode pattern; and (b) cross-section view through the orifice. The electrodes and glass insulator layers were built up on the ceramic substrate using hybrid circuit fabrication techniques.

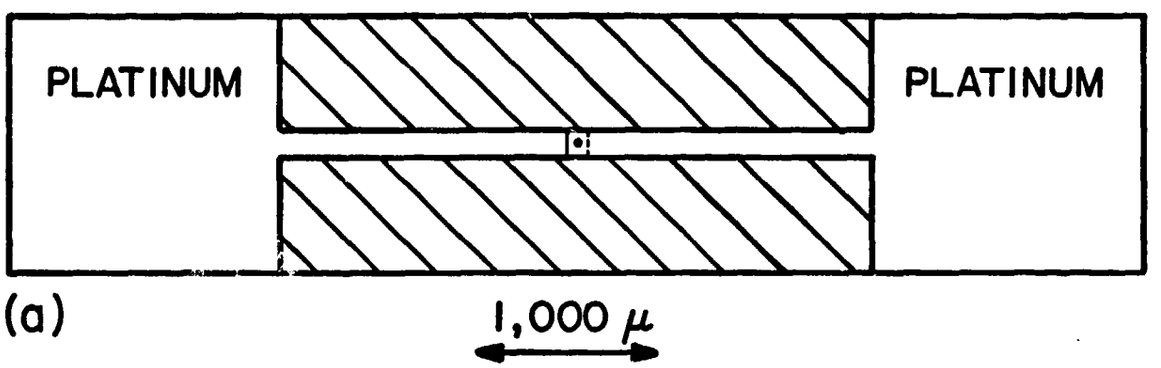

(a)

1,000 μ

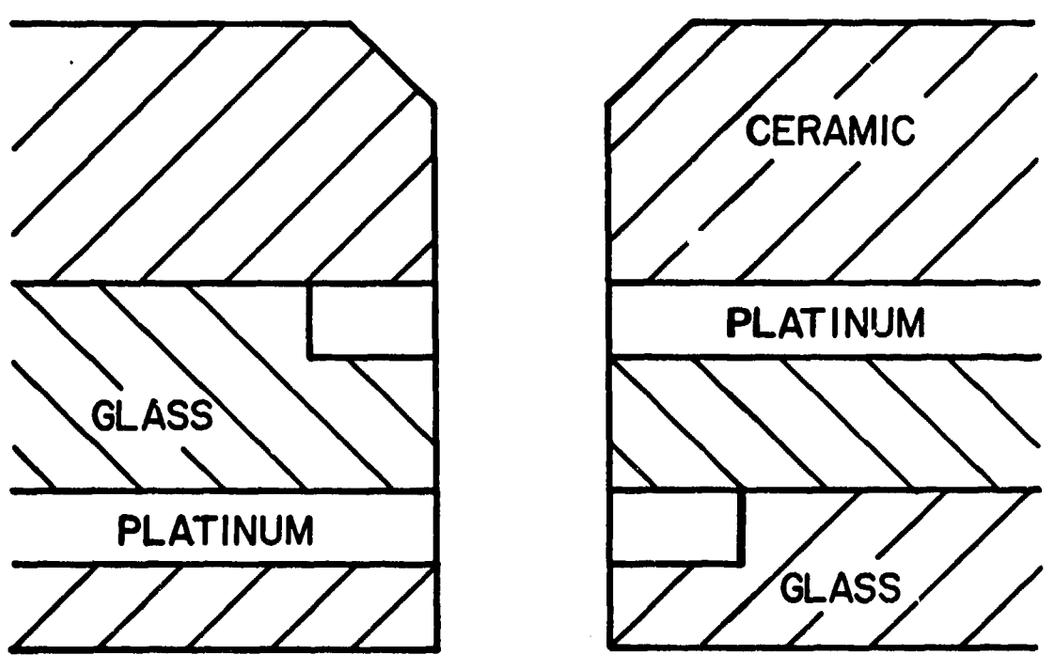

(b)

100 μ

FIG. 5. Examples of pulse-height spectra obtained with the flow-system instrument. Spectra 3a and 3b are the dc Coulter volume and 0° ac pulse spectra, respectively, for 15.7-μm diameter polystyrene spheres. Spectra 3c and 3d are the dc Coulter volume and 0° ac pulse spectra for Chinese hamster ovary (CHO) cells. The frequency for the ac measurements was 1.0 MHz in both cases, and all measurement conditions were identical for the experiments with plastic spheres and CHO cells. The dc and ac measurements were made simultaneously for each particle, and the results were stored in a computer for later analysis.

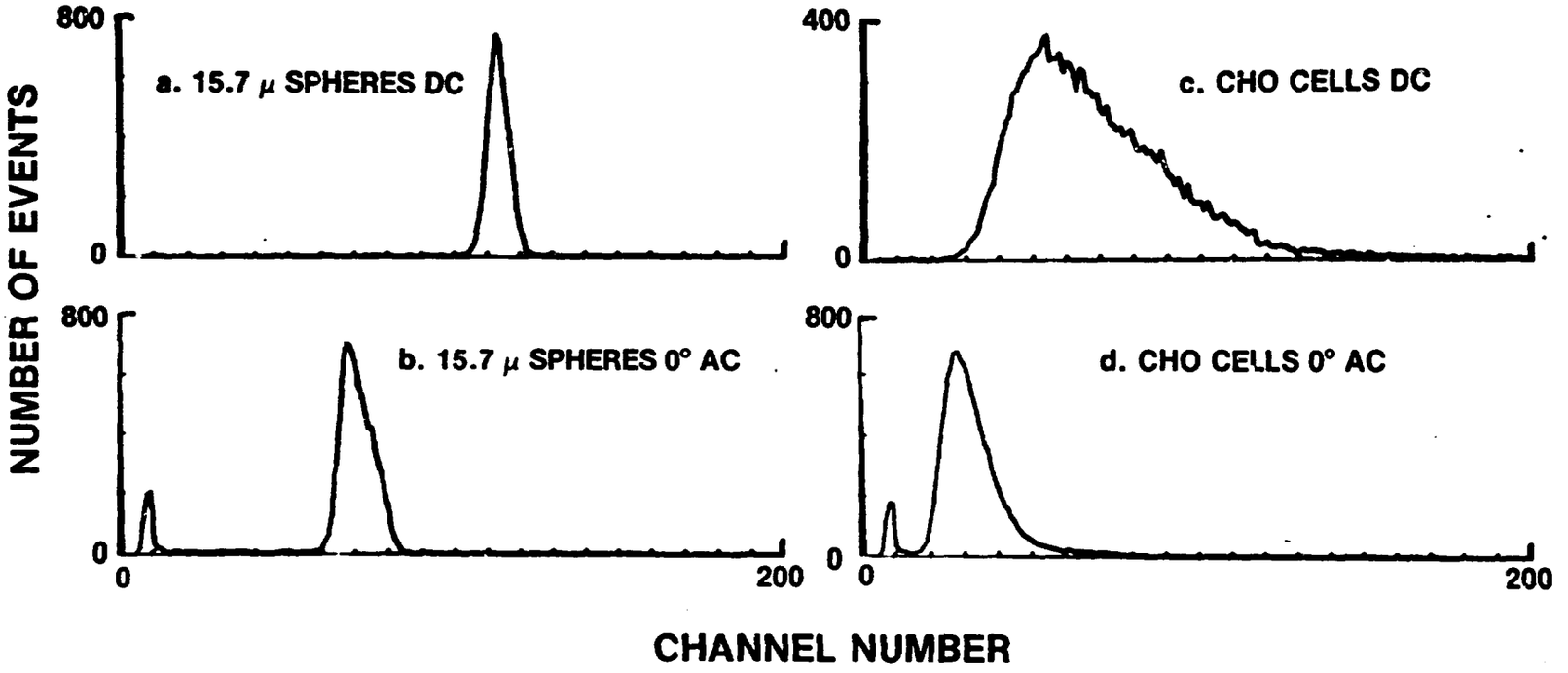
800
a. 15.7 μ SPHERES DC
0
400
c. CHO CELLS DC
0
800
b. 15.7 μ SPHERES 0° AC
0
0
200
800
d. CHO CELLS 0° AC
0
0
200
NUMBER OF EVENTS
CHANNEL NUMBER

FIG. 6. Contour map of the CHO cell data shown in Fig. 5. The contours are for 10, 100, 800 and 1200 events. There is a high correlation between the ac and dc parameters; however, several poorly resolved peaks were observed in the distribution which have not been interpreted. The population shown in the crosshatched region is a small contamination of 15.7-μm plastic spheres from a previous experiment.

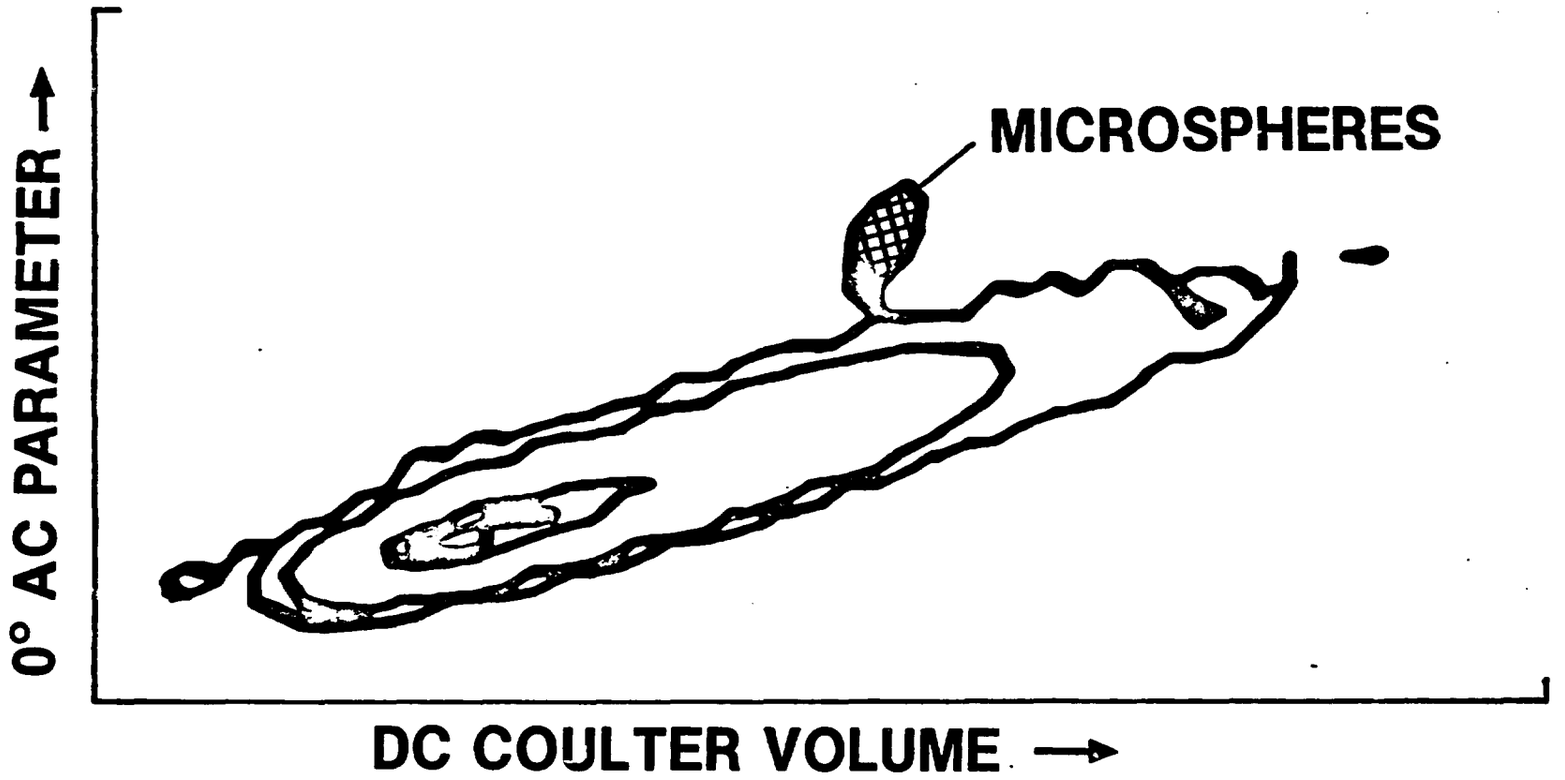
MICROSPHERES
0° AC PARAMETER →
DC COULTER VOLUME →